

Protein Subunits Released by Surface Collisions of Noncovalent Complexes: Nativelike Compact Structures Revealed by Ion Mobility Mass Spectrometry**

Mowei Zhou, Shai Dagan, and Vicki H. Wysocki*

The quaternary structure of proteins determines their biological function, and a majority of proteins exist as oligomers *in vivo* with miscellaneous architectures.^[1] Mass spectrometry (MS) can be applied to study the stoichiometry and interactions of protein complexes by molecular weight measurements under gentle instrumental conditions where noncovalent interactions are preserved in the gas phase.^[2] Recently, there have been extensive efforts to also utilize ion mobility (IM) techniques combined with MS for structural studies of noncovalent biological complexes,^[3] including virus assembly pathways,^[4] because IM provides conformational information, which is not accessible by MS, for these gas-phase ions. Experimentally measured collisional cross sections (CCSs) from IM can serve as constraints for architecture determination by molecular modeling.^[5] Additionally, tandem MS can be used to dissociate gas-phase complexes.^[2b,6] A protein assembly would ideally dissociate into various noncovalent subcomplexes, and the topology of the original complex could be derived by piecing together all the subcomplex products. The common tandem MS method, collision induced dissociation (CID), involves activation of the complexes by collision with neutral gas atoms or molecules. Typically, CID results in an “asymmetric” dissociation into highly charged monomers and complementary ($n-1$)-mers^[7] (although a few exceptions have been reported^[8]), and studies have suggested that unfolding of protein complexes occurs in CID.^[9] It is therefore difficult to relate the CCS measurements of CID product ions to the complexes’ native structure.

Tandem MS can alternatively be achieved by surface induced dissociation (SID) where the complexes collide with a surface target. Previous research in our group^[7,10] has shown that several protein complexes dissociate in a more “symmetric” manner with SID than by CID, and have charge distributed more proportionally to the mass. We hypothesized that dissociation might occur in the absence of gradual monomer unfolding for SID because activation by SID is

a single-step, higher-energy deposition, fast process that is different from the multistep, slower CID process.^[7,10b] SID has recently been applied to determining the quaternary structure of a heterohexameric protein with information from subunit product ions such as heterotrimers unique to SID.^[10a] We present herein the first IM measurements on the SID products of several protein complexes, along with comparison to CID products, by using a modified quadrupole/IM/time-of-flight (Q/IM/TOF) instrument. Briefly, the precursor ions are dissociated by CID or SID cells placed in front of the IM cell. The product ions are subsequently separated based on their size, shape, and charge under the influence of a continuous series of electrical pulses and friction with neutral gas in the IM cell. The drift times of the ions are recorded, with larger and lower-charged ions experiencing longer drift times. Experimental CCSs can be derived from the measured drift times and mass-to-charge-ratios.^[11] Theoretical CCSs can be calculated from crystal structures. Nativelike ions should have experimental CCSs similar to the crystal structure, whereas unfolded ions are expected to show larger CCS values because of an increased surface area.

We first examined the remaining undissociated pentamer precursor of C-reactive protein (CRP) after activation by either CID or SID. Triethylammonium acetate (TEAA) was added in the electrospraying buffer, which has been reported as a charge reducing additive to increase the stability of protein complexes in the gas phase.^[12] Without TEAA no remaining precursor could be observed in SID, even at low acceleration voltages. The addition of TEAA did not cause any remarkable structural change of the protein as the CCSs of the precursor did not change after charge reduction. The +18 precursor of CRP was selected and activated. Examination of precursor CCSs at various SID acceleration voltages (20–50 V) reveals that most of the CRP pentamer dissociated without extensive increase in CCS of the remaining precursor. In CID, however, the CCS of the undissociated CRP pentamer first decreased at low acceleration voltages and then increased considerably above its dissociation threshold of about 80 V. It reached a stable unfolding intermediate with CID around 100 V, where the CCS does not additionally increase with increasing CID acceleration voltages (data not shown). It is impractical to determine one acceleration voltage at which the amounts of the internal energies deposited in CID and SID are identical because of different mechanisms and complications from the physical properties of large protein complexes. Nonetheless, we show here a representative comparison between CID at 100 V (Figure 1, top right) and SID at 40 V (Figure 1, bottom

[*] M. Zhou, Dr. S. Dagan,^[†] Prof. V. H. Wysocki
Department of Chemistry and Biochemistry, University of Arizona
1306 E. University Blvd., Tucson, AZ (USA)
E-mail: vwysocki@email.arizona.edu

[†] Permanent address: Israel Institute for Biological Research (IIBR)
POB 19, Ness Ziona 74100 (Israel)

[**] The authors acknowledge Kevin Giles from Waters Corporation for helpful discussions. We are grateful for the financial support from the National Science Foundation under Grant 0923551.

Supporting information for this article is available on the WWW under <http://dx.doi.org/10.1002/anie.201108700>.

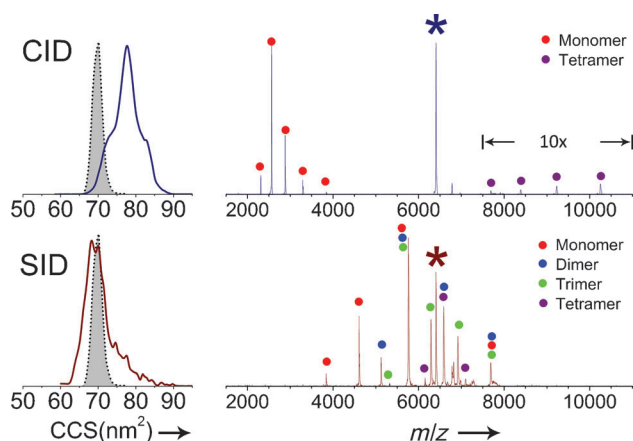


Figure 1. CCS profiles of the remaining CRP pentamer precursor (+18) in CID (top left, blue curve) and SID (bottom left, red curve). The protein was electrosprayed in a mixture of 80 mM ammonium acetate (AA) and 20 mM TEAA. Shaded peaks in each profile are the measured CCS distributions of the pentamer precursor without activation. The corresponding tandem mass spectra of the CRP pentamer in CID (top) and SID (bottom) are shown on the right. Product ions are labeled with colored circles and precursor ions with asterisks.

right), where both spectra exhibit a significant abundance of product ions in presence of the undissociated precursor. Corresponding CCS profiles of the remaining precursor ions after collision are also included in Figure 1. The CCS of the pentamer after collisional activation with gas increases by 11 %, but after collision with a surface it remains centered at almost the same CCS as before collision. The abundance of the undissociated precursor in CID (100 V) is about 46 % of the total ion signal. However, most of the precursor has already dissociated in 40 V SID (14% of total ion abundance), thus implying a higher internal energy deposition in SID in spite of the lower acceleration voltage. Even with the higher internal energy in SID indicated by the greater precursor depletion, no significant change in the CCS of the remaining precursor has been observed, other than some broadening in the CCS distribution. The change in CCS of the undissociated precursor in CID suggests that large-scale structural changes of the precursor occurred prior to complete dissociation in CID, with collapse occurring at lower energies (30–80 V) and expansion at higher energies. In contrast, the precursor remaining after surface activation retained a CCS similar to the original CCS over a range of energies (20–50 V), and presumably a structure that is more similar to the original structure. It is noted that the remaining precursor detected in SID is unlikely to be a result of stray ions which traversed the IM cell without surface collision as based on several experimental observations (see the Supporting Information).

Another critical aspect of this experiment was measurement of the CCS of dominant CID/SID monomer products (Figure 2) of the CRP pentamer (+18), to determine whether the product ions remain compact or unfolded. The CCS profile of CRP monomers denatured in acetonitrile/water/formic acid (50:50:0.1) is also included for comparison. The theoretical CCS of the CRP monomer was calculated by clipping the monomer subunit from the pentameric crystal

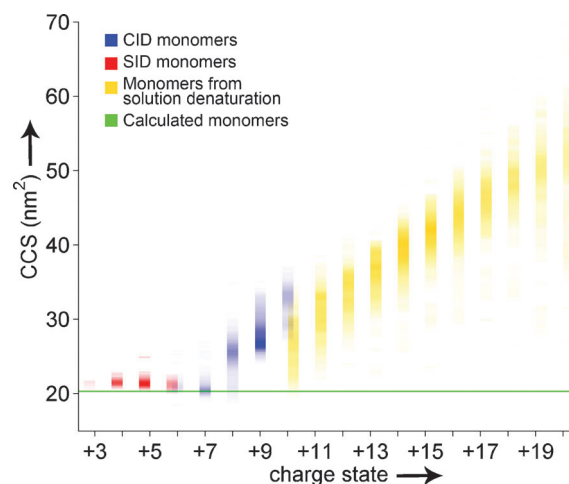


Figure 2. CCS profile of CRP monomer product ions for CID (blue, +6–+10) and SID (red, +3–+6) from a native CRP pentamer precursor, as well as solution denatured CRP monomers (yellow, +10–+20) over different charge states. The green line is the calculated CCS for the CRP monomer clipped from the crystal structure. Color depth of the spots is proportional to the square root of the relative abundance of the species. Monomer product ions in SID are compact and in agreement with monomer CCSs calculated from the crystal structure.

structure. The CCS values of SID monomers are in good agreement with the calculated clipped “native” monomers. Conversely, CID monomers and solution denatured monomers showed increasing CCS with increasing charge. The increase in the CCS in CID is consistent with monomer unfolding. An interesting feature in Figure 2 is that the increase in CCSs with increase in the charge state of the CID monomers tends to follow a trend similar to that of the solution denatured monomers. Also at low-charge states of +6 and +7 the CID monomers are compact and have CCSs similar to SID monomers as well as calculated values, although they are much less abundant in the CID spectrum than in SID. This implies that there is a correlation between charge state and compactness of the gas-phase ions even if the ions are generated with different methods. For larger oligomeric SID products (dimer, trimer, and tetramer) produced from the CRP pentamer (+18), preliminary data indicates that most of them also adopt compact conformations with constant CCSs, independent of the observed charge states. Further investigation with theoretical modeling is required to determine their structures. The same trend in the CCS of monomers can be obtained for the CRP precursor (+24) electrosprayed in 100 mM AA without a charge reducing reagent, except that higher charge states of the monomers were observed in both CID and SID (data not shown).

To examine the generality of our observation on the behavior of CRP monomers, CCS values of monomer product ions from the transthyretin (TTR) tetramer (+15) and serum amyloid P (SAP) pentamer (+24) are shown in Figure 3 for both CID and SID, along with the calculated CCSs for the monomers clipped from crystal structures. Acceleration voltages for CID and SID are 70 V for TTR and 100 V for

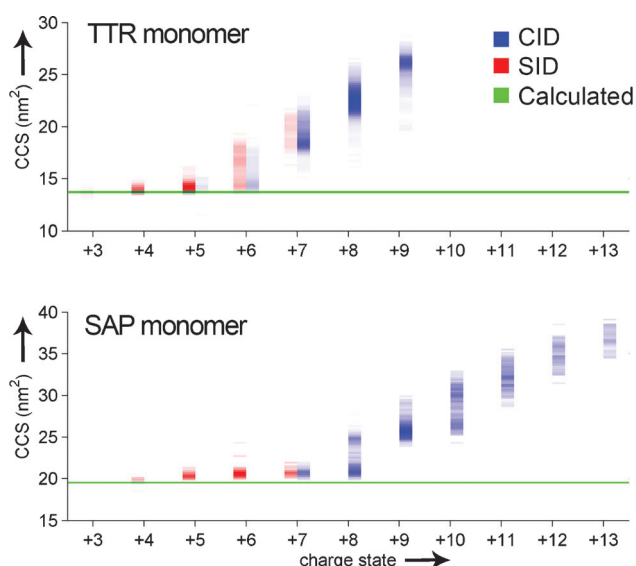


Figure 3. CCS profiles of monomer product ions of different charge states from CID (blue, +6–+9) and SID (red, +3–+7) for TTR tetramer +15 (top), and CID (blue, +7–+13) and SID (red, +4–+7) monomer product ions for SAP pentamer +24 (bottom). Both were electrosprayed in 100 mM AA. Color depth of the spots indicates the relative abundance of the species in a square root scale.

SAP. Generally, the monomers exhibit a trend similar to CRP monomers, where SID monomers have a CCS similar to calculated values and CID monomers show increasing CCS values with an increase in the charge state. It is interesting to note that at intermediate charge states (+5, +6, +7 for TTR and +7 for SAP), CCSs of the CID and SID monomer products largely overlap. This further illustrates that there is a correlation of the charge state and gas-phase structure. In addition, a bimodal distribution of CCSs can be seen for the +6 TTR monomer and +8 SAP monomer, thus suggesting there is a maximum charge state where the ions can still partially keep their compact structure.

In conclusion, this is the first reported evidence from IM measurements showing that dominant SID products are compact and presumably natively like as supported by CCS measurements. In contrast, major CID products, which are usually highly charged monomers, show a gradual expansion in the CCSs with an increasing charge state of the product ions. The CCS values of the more highly charged CID monomers are similar to the values of monomers obtained by solution denaturation. A strong correlation between charge state and CCSs of the unfolded product ions is observed. The compactness of SID monomers as monitored by ion mobility supports our previous hypothesis, based on charge state alone,^[7] that these low-charge product ions are indeed more folded than the higher-charged monomer products in CID. We also show, by using the CRP pentamer, the capability of SID to achieve subunit dissociation of a protein complex prior to extensive unfolding of the precursor. These observations can be rationalized by the rapid, energetic activation in SID which results in less conformational disruption to the protein complexes. In comparison, the slower, multistep, low-energy activation in CID favors structural rearrangement pathways.

The ability to preserve native structures in gas-phase activation is of great importance in the application of mass spectrometry to structural biology. Quaternary structures of protein complexes derived from tandem MS products that are released in their folded form should better reflect the native structure in solution. Several questions, including the effect of charge state on protein unfolding/dissociation and the conformation of oligomeric product ions are under further investigation. Our preliminary results show that multimer product ions which provide more subunit contact information on the protein complexes can be observed by using SID with the lower-charged precursor ions.

Experimental Section

The principle of IM separation in the Q-IM-TOF instrument (Synapt G2, Waters Corporation, UK) has been described previously.^[13] The customized SID device, which was adapted from a previous design^[14] but with smaller dimensions, was inserted between the CID cell and the IM cell (see Scheme S1 in the Supporting Information). Protein samples were purchased from Sigma–Aldrich (USA) and Calbiochem (USA). All native protein samples were buffer exchanged into 100 mM AA with size exclusion chromatography spin columns (Bio-Rad, USA) and diluted to the desired concentration before analysis (20–25 μ M). TEAA was added into the protein solutions for some experiments as indicated in the text. For denatured samples, the protein was first buffer-exchanged into water and then diluted to working concentration with acetonitrile and formic acid. Nanoelectrospray at a capillary voltage of 1.0–1.5 kV and a cone voltage of 50 V was used for all of the experiments. Procedures of glass capillary and surface preparation can be found elsewhere.^[14] Typical instrumental conditions are 5 mbar for the backing pressure, 2 mbar for nitrogen gas pressure in the IM cell, 120 mL min⁻¹ gas flow in the helium cell, 6 \times 10⁻⁷ mbar in the TOF analyzer, and a wave height of 18 V for the traveling wave in the IM cell. The wave velocity was varied for different samples (190–300 ms⁻¹). The voltages in the instrument were tuned to minimize extra activation without compromising transmission. The theoretical CCS values were calculated from crystal structures using the trajectory method in Mobcal.^[15] Further details of the CCS measurement are included in the Supporting Information.

Received: December 10, 2011

Revised: February 10, 2012

Published online: March 21, 2012

Keywords: mass spectrometry · noncovalent interactions · protein folding · protein structures · structural biology

- [1] H.-B. Shen, K.-C. Chou, *J. Proteome Res.* **2009**, *8*, 1577–1584.
- [2] a) F. Sobott, C. V. Robinson in *Principles of Mass Spectrometry Applied to Biomolecules*, Wiley, Hoboken, **2006**, pp. 147–175; b) T. L. Pukala, *Aust. J. Chem.* **2011**, *64*, 681–691.
- [3] C. Uetrecht, R. J. Rose, E. van Duijn, K. Lorenzen, A. J. R. Heck, *Chem. Soc. Rev.* **2010**, *39*, 1633–1655.
- [4] a) C. Uetrecht, I. M. Barbu, G. K. Shoemaker, E. v. Duijn, A. J. R. Heck, *Nat. Chem.* **2011**, *3*, 126–132; b) T. W. Knapman, V. L. Morton, N. J. Stonehouse, P. G. Stockley, A. E. Ashcroft, *Rapid Commun. Mass Spectrom.* **2010**, *24*, 3033–3042.
- [5] A. Politis, A. Y. Park, S.-J. Hyung, D. Barsky, B. T. Ruotolo, C. V. Robinson, *PLoS ONE* **2010**, *5*, e12080.
- [6] A. J. R. Heck, *Nat. Methods* **2008**, *5*, 927–933.
- [7] R. L. Beardsley, C. M. Jones, A. S. Galhena, V. H. Wysocki, *Anal. Chem.* **2009**, *81*, 1347–1356.

- [8] a) R. H. H. van den Heuvel, E. van Duijn, H. Mazon, S. A. Synowsky, K. Lorenzen, C. Versluis, S. J. J. Brouns, D. Langridge, J. van der Oost, J. Hoyes, A. J. R. Heck, *Anal. Chem.* **2006**, *78*, 7473–7483; b) E. B. Erba, B. T. Ruotolo, D. Barsky, C. V. Robinson, *Anal. Chem.* **2010**, *82*, 9702–9710.
- [9] a) J. C. Jurchen, E. R. Williams, *J. Am. Chem. Soc.* **2003**, *125*, 2817–2826; b) I. Sinelnikov, E. N. Kitova, J. S. Klassen, *J. Am. Soc. Mass Spectrom.* **2007**, *18*, 617–631; c) J. L. P. Benesch, J. A. Aquilina, B. T. Ruotolo, F. Sobott, C. V. Robinson, *Chem. Biol.* **2006**, *13*, 597–605; d) S. Sciuto, J. Liu, L. Konermann, *J. Am. Soc. Mass Spectrom.* **2011**, *22*, 1679–1689.
- [10] a) A. E. Blackwell, E. D. Dodds, V. Bandarian, V. H. Wysocki, *Anal. Chem.* **2011**, *83*, 2862–2865; b) C. M. Jones, R. L. Beardsley, A. S. Galhena, S. Dagan, G. Cheng, V. H. Wysocki, *J. Am. Chem. Soc.* **2006**, *128*, 15044–15045.
- [11] a) M. F. Bush, Z. Hall, K. Giles, J. Hoyes, C. V. Robinson, B. T. Ruotolo, *Anal. Chem.* **2010**, *82*, 9557–9565; b) B. T. Ruotolo, J. L. P. Benesch, A. M. Sandercocock, S.-J. Hyung, C. V. Robinson, *Nat. Protoc.* **2008**, *3*, 1139–1152.
- [12] K. Pagel, S.-J. Hyung, B. T. Ruotolo, C. V. Robinson, *Anal. Chem.* **2010**, *82*, 5363–5372.
- [13] a) K. Giles, S. D. Pringle, K. R. Worthington, D. Little, J. L. Wildgoose, R. H. Bateman, *Rapid Commun. Mass Spectrom.* **2004**, *18*, 2401–2414; b) K. Giles, J. P. Williams, I. Campuzano, *Rapid Commun. Mass Spectrom.* **2011**, *25*, 1559–1566.
- [14] A. S. Galhena, S. Dagan, C. M. Jones, R. L. Beardsley, V. H. Wysocki, *Anal. Chem.* **2008**, *80*, 1425–1436.
- [15] a) M. F. Mesleh, J. M. Hunter, A. A. Shvartsburg, G. C. Schatz, M. F. Jarrold, *J. Phys. Chem.* **1996**, *100*, 16082–16086; b) A. A. Shvartsburg, M. F. Jarrold, *Chem. Phys. Lett.* **1996**, *261*, 86–91.